STUDY ON PROBABILISTIC SEISMIC HAZARD MAPS OF TAIWAN AFTER CHI-CHI EARTHQUAKE

Chin-Tung Cheng[1], Shian-Jin Chiou[2], Chyi-Tyi Lee[3], and Yi-Ben Tsai[4]

ABSTRACT

Probabilistic seismic hazard maps are widely used for engineering design, land use planning, and disaster mitigation *etc*. This study conducted a review of readily available information on tectonic setting, geology, and seismicity, and the attenuation of peak ground acceleration (PGA) of Taiwan for completing the revised probabilistic seismic hazard maps by the state-of-the-art probabilistic seismic hazard analysis (PSHA) method. The mainshocks from the earthquake catalog of 1900 to 1999 were used to evaluate the earthquake recurrence rate for regional sources and subduction-intraslab sources from Truncated-Exponential model. The fault-slip rates for estimating the earthquake recurrence rates of faults and subduction interface sources by Characteristic-Earthquake model were adopted. The revised PSHA in this study takes into consideration the fact that subduction plate sources induce higher ground-motion levels than crustal sources, and active faults induce the hanging-wall effect in attenuation relationships. After considering the fault activity and hanging wall effects in our revised PSHA, it was found that the peak ground acceleration (PGA) levels of near-field in Taiwan always exceed 0.4 g in a 475-year return period. This situation is clearly obvious in central Taiwan, the Miaoli-Taichung region, Chyiayi-Tainan region and eastern longitudinal valley.

Key words: Probabilistic seismic hazard, fault, ground motion.

1. INTRODUCTION

Before the occurrence of Chi-Chi earthquake, the results of Probabilistic Seismic Hazard Analysis (PSHA) produced by different agencies and researchers almost universally underestimated earthquake hazards in Central Taiwan. Therefore, the Chi-Chi earthquake has the following impacts on PSHA:

(1) Saturation of local magnitude: The Chi-Chi earthquake indicates that local magnitude (M_L) is saturated at a large magnitude. Moment magnitude (M_W) should be used instead.

(2) Significant hanging wall effect: It shows much higher ground motion amplitude at hanging wall than at footwall during Chi-Chi earthquake. Therefore, the hanging wall effect should be considered for certain faults.

(3) The need to emphasize the fault source: Before the occurrence of Chi-Chi earthquake, the results of PSHA underestimated earthquake hazards in Central Taiwan. The situation was due to improper handling of fault source.

(4) The need to use the closest-distance to fault plane: When a large earthquake with long rupture occurs, using hypocenter distance is no longer valid, and using closest-distance to surface rupture line is also inappropriate. Instead, the close-distance to fault plane should be used, so that a better attenuation relationship can be obtained.

After Chi-Chi earthquake, the need to emphasize the fault source was recognized, and the need to adopt a proper attenuation relationship while considering the strong-motion data recorded in the Chi-Chi earthquake sequence for PSHA usage. In this study, a review of readily available information on attenuation of peak ground acceleration, tectonic setting, geology, active faults, and seismicity of Taiwan for PSHA was made. In this paper, the general methodology of PSHA and the basis of inputs to the PSHA are summarized, with emphasis on seismic sources judged to be most significant to the seismic hazard in Taiwan. After considering the fault activity in the revised PSHA, seismic hazard maps of Taiwan in a 475 and 2475-year return periods are presented.

Manuscript received December 8, 2006; revised April 3, 2007; accepted April 4, 2007.

[1] Researcher (corresponding author), Sinotech Engineering Consultants, Inc., Taipei, Taiwan 110, R.O.C.

[2] Researcher, Sinotech Engineering Consultants, Inc., Taipei, Taiwan 110, R.O.C. (e-mail: chiu@sinotech. org.tw).

[3] Associate Professor, Institute of Applied Geology, National Central University, Taoyuan County, Taiwan 32001, R.O.C.

[4] Researcher, Pacific Gas and Electric Company, San Francisco, CA 94105-1126, U.S.A.

2. PSHA METHODOLOGY

2.1 Basics of PSHA Methodology

The methodology used to conduct a PSHA was developed first by Cornell (1968) and has undergone substantial development since that time. Current practice is described in detail in several publications, such as the National Research Council (1988), Earthquake Engineering Research Institute (1989), and Coppersmith (1991). The theory of PSHA involves computing the annual frequency at which a ground motion parameter exceeds a specified level at the site of interest termed the hazard curve. The probability of exceeding ground motion amplitude in a given period of time is related to annual frequency of exceedance by the equation (Cornell, 1968):

$$P(Z > z \mid T) = 1 - e^{-v(z)T} \le v(z)\,T \tag{1}$$

where $P(Z > z|T)$ = probability of exceedance during a time period (T) and $v(z)$ = annual frequency of exceedance.

The often-used term "return period" is the reciprocal of annual frequency of exceedance ($1/v$). The annual frequency of exceedance is computed by the equation:

$$v(z) = \sum_{n=1}^{N} \sum_{m=m_0}^{m_u} \lambda_n(m_i) \left[\sum_{r_j=0}^{r_{\max}} P_n(R = r_j \mid m_i) P(Z > z \mid m_i, r_j) \right] \quad (2)$$

where

$\sum^{N}$ = summation over all (N) seismic sources;

$\lambda_n(m_i)$ = the annual frequency of occurrence of earthquakes of magnitude m_i on seismic source n;

$P_n(R = r_j | m_i)$ = the probability of an earthquake of magnitude m_i on source n occurring at a closest distance r_j from the site;

$P_n(Z > z | m_i, r_j)$ = the probability of ground motion Z exceed a specified value z at an earthquake magnitude m_i and the shortest distance r_j from the site;

m_i is between lower-bound magnitude m_0 and upper-bound magnitude m_u.

The calculation of the annual frequency of exceedance involves: (1) computing the frequency of occurrence of events of magnitude m_i on source n; (2) calculating the probability distribution for the distance from the site to events of magnitude m_i, on source n; and (3) computing the probability that an event of magnitude m_i will exceed the specified ground motion level, z. Summing over all distances for a given magnitude, and over all event magnitudes then obtains the total rate of exceedance.

In this study, PSHA considered uncertainty in defining the models and parameters that are most appropriate for performing the analysis. A logic tree approach was used to incorporate credible alternatives for seismic source interpretations, seismic source parameters, and ground motion attenuation models.

2.2 Procedure of PSHA

Figure 1 is the procedure of PSHA in this study. The four major elements of the probabilistic procedure are (1) the characterization of seismic sources; (2) the characterization of attenuation of ground motion, (3) the actual calculation of probabilities, and (4) the production of PSHA. First of all, the earthquakes and active faults related databases were incorporated into GIS (Geographic Information System), then the regional sources divided, and source models were selected. There are two models to estimate the recurrence rate of earthquakes. One is the Truncated-Exponential model (Cornell and Van Marke, 1969), and the other is the Characteristic-Earthquake model (Youngs and Coppersmith, 1985). Secondly, Strong ground motion attenuation relationships were developed according to the Taiwan strong motion data including Chi-Chi earthquake sequences and some global records with large magnitude. The characteristic parameters of each source were calculated and the appropriate attenuation relationships adopted. Thirdly, a logic tree was adopted to deal with the uncertainties of parameters in PSHA, such as: source type, attenuation relationship, focal depth, earthquake magnitude distribution model, and fault geometry, and finally, not only ground motion hazard curves, probabilistic seismic hazard maps were obtained, but also uniform hazard response spectrum and deaggregation.

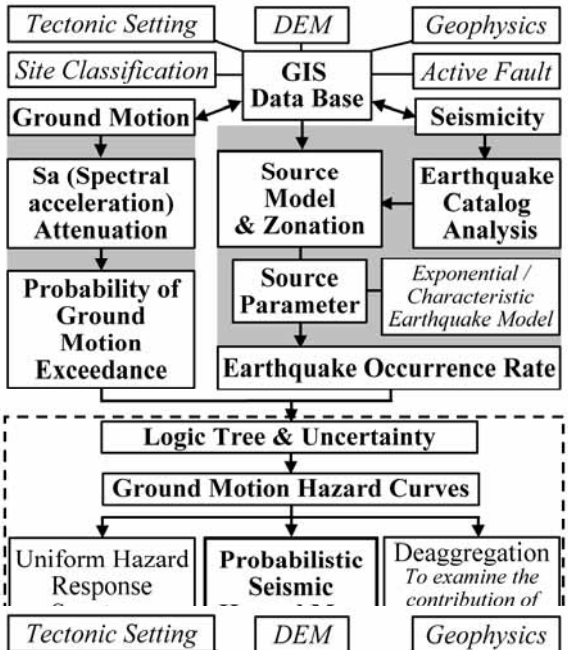

Fig. 1 Procedure of probabilistic seismic hazard analysis

3. TECTONIC SETTING AND SEISMICITY

3.1 Tectonic Setting

The island of Taiwan is situated at the junction of the Ryukyu and Philippine arcs. According to the plate tectonics, most of the island is on the eastern border of the Eurasian plate, whereas the Coastal Range in eastern Taiwan is on the western edge of the Philippine Sea plate (Tsai, *et al*., 1977). The arc-continent collision, starting in the Late Miocene period, has produced the highly deformed terrain of Taiwan and the resulting compressional stresses have created intense folding and thrusting in the mountain belt. Due to the oblique nature of the collision, thrusting and folding started earlier in northeastern Taiwan and gradually propagated to central and southern Taiwan, where present-day active crustal deformation and earthquakes are located. Contrary to central and southern Taiwan, northern Taiwan now shows a different tectonic setting from that of the main collision zone. Due to the tectonic stress transmitted to western Taiwan, seismic activity in this area is quite frequent.

3.2 Taiwan Seismicity

The sources of earthquake catalogue include historical records and instrumented earthquake data. To review historical seismicity, we used the catalog of pre-instrumented earthquakes compiled by Cheng and Yeh (1989). This catalog provides a list of historical earthquakes dating back as early as 1604. The information sources of the earthquake catalogs are from Central Weather Bureau Seismic Network, operated by the Central Weather Bureau, and the Taiwan Telemetry Seismic Network, operated by the Institute of the Earth Sciences, Academia Sinica. The earthquake epicenter maps in Taiwan from 1900 to 2005, $M_w \geq 5$, are shown in Fig. 2. The deep earthquakes occur mostly in northeastern Taiwan, where earthquake occurrence is closely related to the subduction of the Philippine Sea plate under the Eurasian plate along the Ryukyu Trench. It should be noted that, there were several damage earthquakes accrued in Taipei, Miaoli-Taichung, Chyayi-Tainan, and Hwalian region in the past four centuries (Cheng and Yeh, 1989).

There are several other earthquake catalogs for Taiwan, but

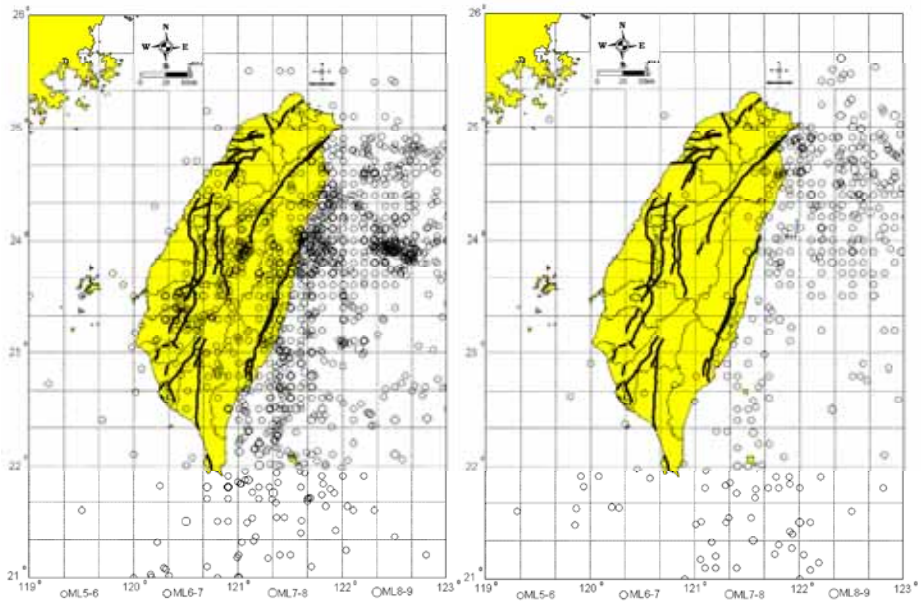

Fig. 2 Earthquake epicenter maps in Taiwan from 1900 to 2005

these catalogs used either local magnitude (M_L) or surface-wave magnitude (M_S). The moment magnitude (M_W) is preferred for our seismic hazard analysis because M_W is more physically based and is the magnitude scale used in recent ground-motion attenuation relationships.

4. SEISMIC SOURCES

In this study, there are four major source types in Taiwan, they are (a) regional source, (b) crustal fault source, (c) subduction plate interface source and (d) subduction plate intraslab source. 3-D plate was adopted to model crustal faults and subduction zone plate geometry in PSHA. Truncated-Exponential model developed by statistics of mainshock catalog in M_W was used to describe the magnitude distribution of regional sources and subduction plate intraslab sources; Characteristic-Earthquake model developed by fault-slip rate was used to describe the magnitude distribution of active fault and subduction interface sources. The characterization of these four seismic sources and their source parameters used Cheng (2002) as reference. Further informations on these seismic sources used are given below.

4.1 Regional Sources

According to the Moho discontinuity and distribution of seismicity, the boundary between shallow and deep regional sources is located at average depths between 30 and 35 km (Yeh and Tsai, 1981; Tsai, 1986; Tsai, *et al.,* 1987; Hetland and Wu, 2001). Hence, the shallow and deep regional sources were separated by the depth of 35 km (Loh, *et al.,* 2002). Furthermore, according to the layers of tectonic framework, seismogenic zone, neotectonic architecture (Shyu, *et al.,* 2005; Tsai, *et al.,* 1986), the active fault distribution (Lin, *et al.,* 2000; Lee, 1999), the epicenter distribution of the past large earthquake of Taiwan, focal mechanism, Bouguer gravity anomalies, geology map, and topography map by GIS were overlaped, then divided into several regional sources. Hence, 21 shallow regional zones and 7 deep regional zones were divided as shown in Figs. 3 and 4.

4.2 Crustal Faults Sources

Due to lack of active fault parameters, previous PSHA studies in Taiwan always used Type III source model (no fault location) (Loh and Jean, 1993; Cheng, 1996). Recent studies of active faults collected for PSHA in this study. TYPE I source model (fault location well-known) was adopted to model the geometries and characteristic parameters of each fault (see Fig. 5). Table 1 lists the details of active faults. Uncertainties in the seismic source parameters are incorporated into PSHA using a logic-tree approach as described in section 6.

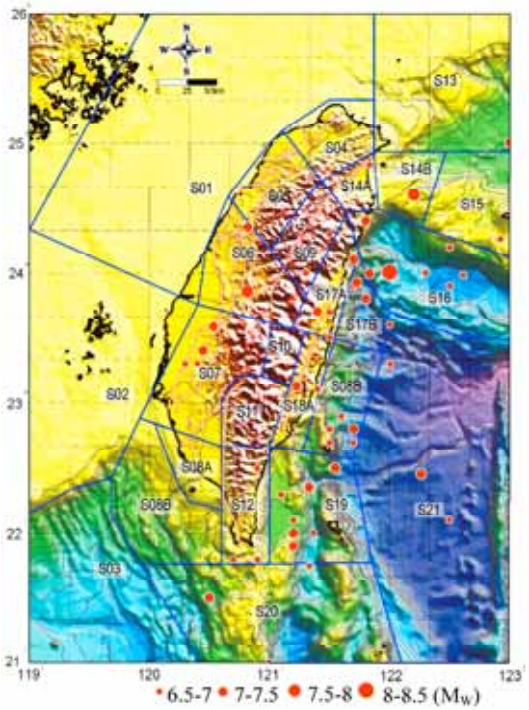

Fig. 3 Shallow regional source division map (S01-S21, depth ≤ 35 km)

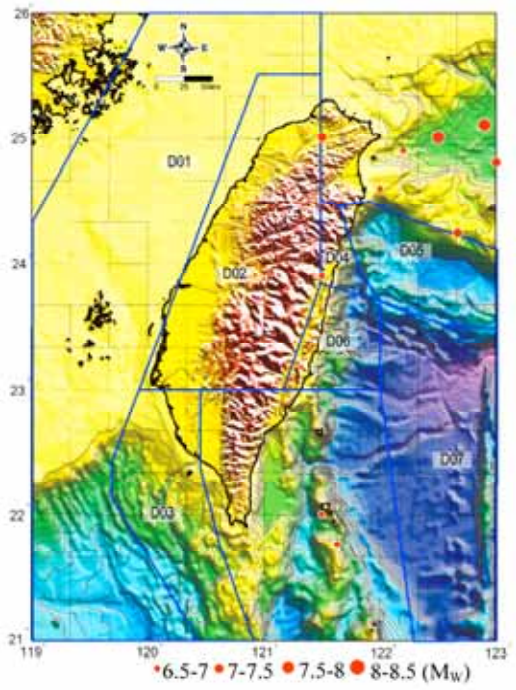

Fig. 4 Deep regional source division map (D01-D07, depth > 35 km)

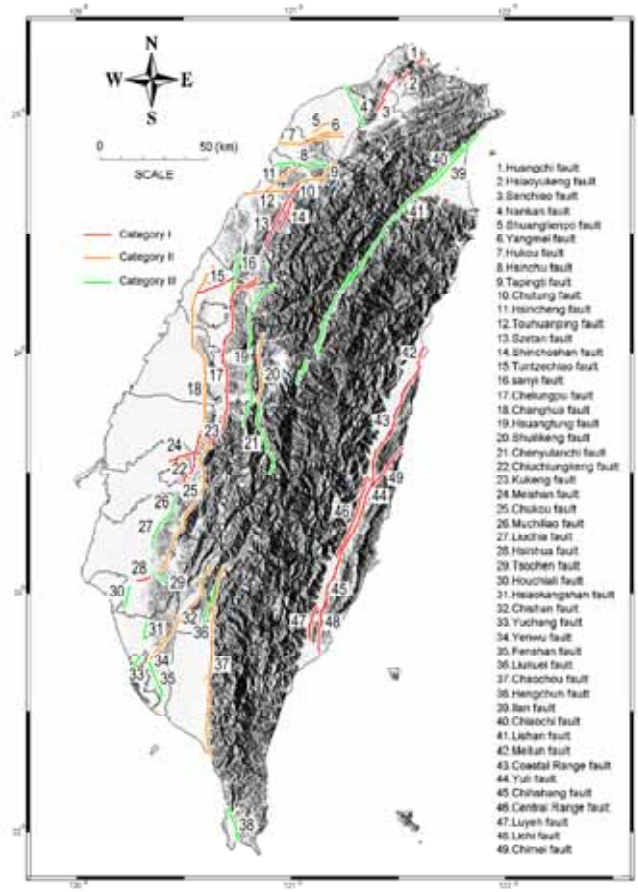

Fig. 5 Active fault map (Lee, 1999)

The recurrence rates of earthquakes on crustal faults sources were estimated from maximum magnitude and slip rate of the faults by using the Characteristic-Earthquake model. The maximum magnitude of earthquake that may occur in these active faults can be estimated using the empirical relations of fault length versus magnitude or fault rupture area versus magnitude given by Wells and Coppersmith (1994). Furthermore, the long-term slip-rate of the active fault is defined as T/D (Schwartz and Coppersmith, 1984), in witch T is the recurrence interval of big earthquakes and D is the slip displacements of fault. Both of them are measured from the trenching of the active fault scarp and paleo-earthquake study. If no trenching information were available for estimating the long-term slip rate, the alternative way for rough evaluating T and D was obtained from geologic map, and deep-wells for geological age and the off-set of the strata on both side of the active fault. The GPS horizontal velocity field could produce short-term slip rate for examining the long-term slip rate (Yu, *et al.*, 1997). The summation of slip rates of the active faults on west coast plain and eastern longitudinal valley of Taiwan island could not be larger than the movement rate (7 ~ 8 cm/year) of Philippine sea-plate moving toward Taiwan island. The slip rate of active faults in Taiwan estimated by Lee (1999) and Cheng (2002) were adopted in this study.

There are a lot of active faults in Taiwan island, therefore the shallow regional source almost includes the seismicity of active faults. In order to avoid double counting the seismicity rate in PSHA, the events $M_W < 6.5$ were treated as background seismicity without relating to any active faults. Adversely, the events $M_W \geq 6.5$ were assumed to be associated with some active faults (see Fig. 6).

4.3 Subduction Plate Intraslab Sources

Figure 7 presents the iso-depth contour of the top of subduction plate and spatial distribution of independent deep earthquakes (focal depth ≥ 35 km) in north-eastern and southern Tai-

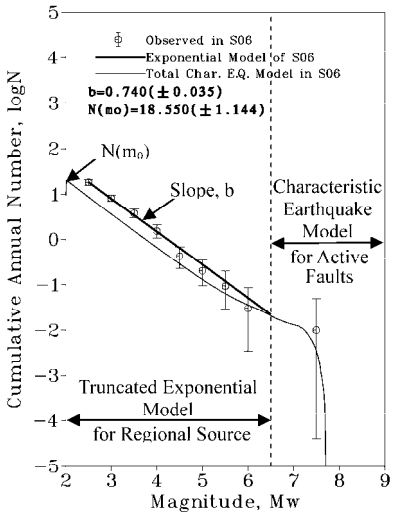

Note:

1. The b-value is the slope of a straight line relating absolute or relative frequency to earthquake magnitude, the Gutenberg-Richter recurrence relationship (log N = a – bM).
2. $N(m_0)$ is the frequency of occurrence of events of magnitude m_0 and larger.

Fig. 6 Recurrence rate of background seismicity ($M_W < 6$) in S06 regional source and large earthquakes induced by faults located in S06

wan. The locations of subduction plate intraslab sources (intraslab NP1-NP9 and SP1-SP3) are also shown in Fig. 7. The maximum magnitudes of intraslab sources were estimated from the records of the global subduction plates (Isacks and Molnar, 1971; Fujita and Kanamori, 1981).

Due to Philippine sea plate being beneath and moving north toward Eurasian plate, the seismicity distribution along the Benioff zone is very significant. Taipei metropolis is located above the north-eastern subduction plate intraslab source. The sources will influence the seismic hazard level of greater Taipei region significantly.

4.4 Subduction Plate Interface Sources

In typical subduction zones, the plate interface is the locus of the plate boundary of coseismic deformation and is the location of the largest earthquakes observed worldwide. From the seismicity data, Kao, *et al*. (1998) inferred that the plate interface located between Ryukyu arc and Taiwan has a variable dip angle and spans the depth from 15 to 35 km. The largest reported earthquake in this portion of the T01 plate interface (shown in Fig. 7) during the past 100 years is a M_W 8.2 earth quake that occurred in 1920. Because the nature of this earthquake is not clear, there is an uncertainty that whether $M_W \geq 8$ events ever occurred along this segment of the interface or not. On the other hand, Kao (1998) argued that the southernmost Ryukyu arc-Taiwan region is unlikely to generate $M_W \geq 8$ interface earthquakes. It was estimated that the maximum magnitude of future events which might rupture in this segment of the interface to be in the range of M_W 7.6 to M_W 7.7. However, the possibility that $M_W \geq 8$ earthquakes may occur along the plate interface were considered in this study.

Table 1 Assessment of the parameters of Taiwan active faults for PSHA

No.	Fault name	Strike	Dip (degree)	Fault mechanism	Length (km)	Depth (km)		Ruptuer width (km)	Displace-ment (m)	Ruptuer area (km^2)	Slip rate (mm/year)	Maximun magnitude, m_u (Mw)	Recurrence interval (year)		
						Top	Button						Younngs & Coppersmith, 1985	Matsuda, 1975	Bolina, 1970
01 + 02 +	Huangchi + Hsiaoyu-	NNE	60SE	Norma & Sinistral	36	0	15	17	1.8	624	2.0 ± 1.0	7.0 ± 0.2	543	746	568
04	Nankan	NNW	80NW	Normal & Dextral	22	0	10	10	0.7	223	0.4 ± 0.2	6.5 ± 0.2	1352	1896	1492
05	Shuanglienpo	ENE	50SE	Reverse	12	2	10	10	0.4	125	0.5 ± 0.25	6.2 ± 0.2	567	1036	831
06	Yangmei	ENE	50NW	Reverse	20	2	10	10	0.8	261	0.5 ± 0.25	6.6 ± 0.2	1082	1704	1334
07	Hukou	ENE	45SE	Thrust	32	0	12	17	1.5	543	1.0 ± 0.5	6.9 ± 0.2	733	1362	1041
08	Hsinchu	E-W	45S	Thrust	28	0	12	17	1.4	475	1.5 ± 0.75	6.8 ± 0.2	395	832	639
09	Tapingti	NNE	45SE	Thrust	15	0	12	17	0.8	255	0.6 ± 0.3	6.5 ± 0.2	653	1378	1080
10	Chutung	NE	50SE	Reverse	14	0	12	16	0.7	219	0.6 ± 0.3	6.5 ± 0.2	760	1249	983
11	Hsincheng	N40E	45SE	Thrust	22	0	12	17	1.1	373	2.0 ± 1.0	6.7 ± 0.2	267	532	412
12	Touhuanping	E-W	80S	Dextral	27	0	12	12	1.0	329	2.5 ± 1.25	6.7 ± 0.2	242	392	304
13	Seztan	N10E	75W	Reverse	35	0	12	12	1.3	435	2.5 ± 1.25	6.8 ± 0.2	259	471	362
14	Shinchoshan	N10E	60E	Reverse	16	0	12	14	0.7	222	2.5 ± 1.25	6.5 ± 0.2	180	302	238
14 BT	Miaoli blind thrust	N10E	30E	Reverse & Dextral	37	2	15	26	2.6	962	5.0 ± 2.5	7.2 ± 0.2	223	397	298
15	Tuntzechiao	N60E	90	Dextral	20	0	15	15	0.9	300	2.5 ± 1.25	6.6 ± 0.2	226	368	287
16	Sanyi	NNE	40E	Thrust	22	0	15	23	1.5	513	1.0 ± 0.5	6.9 ± 0.2	940	1313	1005
17	Chelungpu	N-S	40E	Thrust	90	0	20	31	6.8	2800	15.0 ± 7.5	7.7 ± 0.2	182	268	194
18	Changhua	NNS	30E	Thrust	85	2	15	28	5.4	2354	15.0 ± 7.5	7.6 ± 0.2	153	226	165
19	Tamopu-Hsuangtung	N-S	45E	Thrust	70	0	15	21	3.8	1485	0.8 ± 0.4	7.4 ± 0.2	2282	3306	2444
20	Shuilikeng	N-S	50E	Thrust	32	0	15	20	1.8	627	0.6 ± 0.3	7.0 ± 0.2	1810	2495	1898
21	Chenyulanchi	N-S	50E	Thrust	36	0	15	20	2.0	705	0.8 ± 0.4	7.0 ± 0.2	1207	2023	1533
22	Chiuchiungkeng	NNE	35E	Thrust	24	0	15	26	1.8	628	10.0 ± 5.0	7.0 ± 0.2	109	150	114
23	Kukeng	NW	90	Sinistral	10	0	15	15	0.5	161	3.0 ± 1.5	6.3 ± 0.2	136	204	162
24	Meishan	N75E	90	Dextrtal	14	0	15	15	0.7	216	6.0 ± 3.0	6.5 ± 0.2	94	124	98
24BT	Chaiyi blind thrust	N10E	30E	Thrust	36	2	15	26	2.5	936	12.0 ± 6.0	7.2 ± 0.2	122	163	122
25	Chukou	NE	40E	Thrust	70	0	15	25	4.5	1745	10.0 ± 5.0	7.5 ± 0.2	221	298	219
26 + 27	Muchiliao + Liuchia	NNE	35SE	Thrust	30	0	15	26	2.2	785	8.0 ± 4.0	7.1 ± 0.2	155	217	164
28	Tsochen	NW	90	Sinistral	12	0	15	15	0.6	180	2.5 ± 1.25	6.4 ± 0.2	192	263	209
29	Hsinhua	N70E	90	Dextrtal	12	0	15	15	0.6	180	5.0 ± 2.5	6.4 ± 0.2	96	132	104
30	Houchiali	NNE	60W	Thrust	12	0	15	17	0.7	208	5.0 ± 2.5	6.4 ± 0.2	83	145	114
30BT	Tainan blind thrust	N10E	30E	Thrust	36	2	15	26	2.5	936	10.0 ± 5.0	7.2 ± 0.2	146	195	146
31	Hsiaokangshan	NNE	50SE	Reverse	12	0	15	20	0.7	235	1.5 ± 0.75	6.5 ± 0.2	347	523	411
32	Chishan	NE	45E	Thrust	60	0	15	21	3.3	1273	3.0 ± 1.5	7.3 ± 0.2	507	796	592
33	Yuchang	NE	50E	Reverse	12	0	12	16	0.6	195	1.0 ± 0.5	6.4 ± 0.2	437	694	548
34 + 35	Yenwu + Fenshan	NW	50E	Reverse	21	0	12	16	1.0	329	1.5 ± 0.75	6.7 ± 0.2	487	653	507
36	Liukuei	NE	50E	Reverse	20	0	15	20	1.2	392	0.5 ± 0.25	6.7 ± 0.2	1229	2196	1697
37a	Chaochou (north)	N-S	50E	Reverse	55	0	20	26	3.7	1436	4.0 ± 2.0	7.4 ± 0.2	471	647	479
37b	Chaochou (south)	N-S	50E	Reverse	40	0	20	26	2.8	1044	3.0 ± 1.5	7.2 ± 0.2	433	699	523
38	Hengchun	NNW	50E	Reverse	40	0	20	26	2.8	1044	2.0 ± 1.0	7.2 ± 0.2	650	1048	784
39	llan	NE	60SE	Normal	30	0	15	17	1.5	520	1.5 ± 0.75	6.9 ± 0.2	623	882	675
40	Chiaochi	NE	60SE	Normal	25	0	15	17	1.3	433	2.0 ± 1.0	6.8 ± 0.2	397	587	452
41a	Lishan (a)	NNE	60E	Normal	30	0	15	17	1.5	520	1.5 ± 0.75	6.9 ± 0.2	623	882	675
41b	Lishan (b)	NNE	60E	Normal	25	0	15	17	1.3	433	1.2 ± 0.6	6.8 ± 0.2	666	978	753
41c	Lishan(c)	NNE	60E	Normal	30	0	15	17	1.5	520	1.0 ± 0.5	6.9 ± 0.2	940	1323	1013
41d	Lishan(d)	NNE	60E	Normal	30	0	15	17	1.5	520	1.0 ± 0.5	6.9 ± 0.2	940	1323	1013
42	Meilun	N30E	50E	Reverse & Sinistral	30	0	30	39	3.1	1175	20.0 ± 10.0	7.3 ± 0 2	83	113	84
43	Ueimei	N30E	50E	Reverse & Sinistral	45	0	30	39	4.5	1762	20.0 ± 10.0	7.5 ± 0.2	111	148	109
44	Yuli	N30E	50E	Reverse & Sinistral	48	0	30	39	4.7	1880	16.0 ± 8.0	7.5 ± 0.2	130	193	142
45	Chihshang	N25E	50E	Reverse & Sinistral	30	0	30	39	3.1	1175	20.0 ± 10.0	7.3 ± 0.2	83	113	84
46	Yuli West	NNE	50W	Reverse & Sinistral	40	0	25	33	3.4	1305	10.0 ± 5.0	7.3 ± 0.2	150	243	180
47	Luyeh	N-S	50E	Reverse	18	0	25	33	1.7	587	8.0 ± 4.0	6.9 ± 0.2	105	179	137
48	Lichi	N-S	50E	Reverse & Sinistral	24	0	25	33	2.2	783	16.0 ± 8.0	7.1 ± 0.2	78	108	82
49	Chimei	N40E	50E	Reverse & Sinistral	25	0	30	39	2.6	979	4.0 ± 2.0	7.2 ± 0.2	354	502	377
50	Yueikangshan	N70E	80S	Reverse & Sinistral	12	0	10	12	0.5	139	1.0 ± 0.5	6.2 ± 0.2	312	554	443

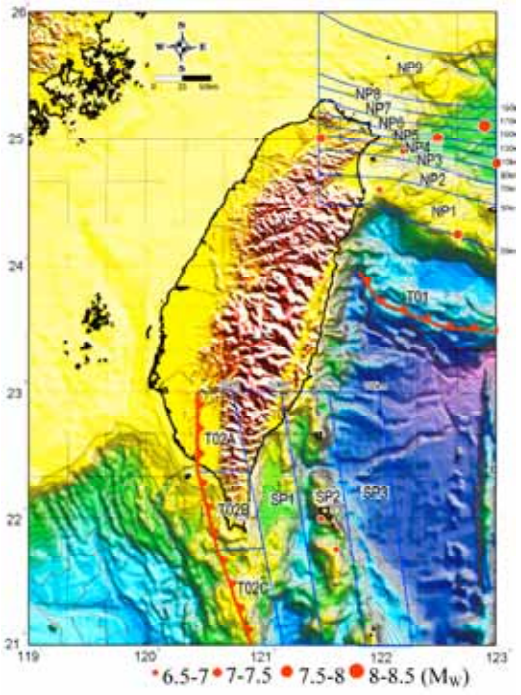

Fig. 7 Subduction plate source division map

5. GROUND MOTION ATTENUATION

Ground motion attenuation relationships applicable to soil or rock conditions were selected to predict PGA for PSHA. The hanging wall effects of certain faults, the characteristics of crustal and subduction zone sources and site classification of strong-motion stations (Lee, *et al.,* 2001) were considered in the ground-motion attenuation relationships used in this PSHA (as shown in Table 2). There are different ground-motion attenuation relationships for different types of source, such as crustal, interface and interslab (subduction zone) earthquakes (Cheng, 2002; Lin, 2002). In this study, the attenuation relationships by Cheng (2002) were used for crustal earthquakes, and those by Lin (2002) were used for subduction zone earthquakes. Comparisons of the predicted median PGA from Table 2, and the attenuation relationships of Tsai, *et al.* (1987), NCREE (1999), and Youngs, *et al.* (1997) are shown in Fig. 8.

The attenuation relationship of Tsai, *et al.* (1987) and NCREE (1999) was derived from Taiwan strong-motion data, including 1999 Chi-Chi earthquake. It had no site classification, and magnitude in the relationship was not M_W, but M_L. Additionally, attenuation relationships of subduction zone sources of Youngs, *et al.* (1997) was derived from global data sets, including data from Japan, Mexico, and Chile. The attenuation rela-

Table 2 PGA attenuation relationships for Taiwan

Specific	PGA attenuation relationship	$\sigma_{\ln y}$	Reference
Hanging wall, Rock, Crustal zone	$\ln y = -3.25 + 1.075\ M_W - 1.723 \ln (R + 0.156 \exp (0.62391\ M_W))$	0.577	Cheng (2002)
Hanging wall, Soil, Crustal zone	$\ln y = -2.80 + 0.955\ M_W - 1.583 \ln (R + 0.176 \exp (0.603285\ M_W))$	0.555	
Foot wall, Rock, Crustal zone	$\ln y = -3.05 + 1.085\ M_W - 1.773 \ln (R + 0.216 \exp (0.611957\ M_W))$	0.583	
Foot wall, Soil, Crustal zone	$\ln y = -2.85 + 0.975\ M_W - 1.593 \ln (R + 0.206 \exp (0.612053\ M_W))$	0.554	
Interface, Rock, subduction zone	$\ln y = -2.5 + 1.205\ M_W - 1.905 \ln (R + 0.51552 \exp (0.63255\ M_W)) + 0.0075\ H$	0.526	Lin (2002)
Interface, Soil, subduction zone	$\ln y = -0.9 + 1.000\ M_W - 1.900 \ln (R + 0.99178 \exp (0.52632\ M_W)) + 0.004\ H$	0.627	
Intraslab, Rock, subduction zone	$\ln y = -2.5 + 1.205\ M_W - 1.905 \ln (R + 0.51552 \exp (0.63255\ M_W)) + 0.0075\ H + 0.275$	0.526	
Intraslab, Soil, subduction zone	$\ln y = -0.9 + 1.000\ M_W - 1.900 \ln (R + 0.99178 \exp (0.52632\ M_W)) + 0.004\ H + 0.31$	0.627	

Note: 1. M_W = moment magnitude; R = closest distance to fault rupture plane (km); H = focal depth (km); y = PGA (g).
2. According to the site classification defined in Uniform Building Code (1997) and Lee *et al.* (2001), rock site included class B (rock) and C (soft rock or very dense soil), and soil site included class D (stiff soil) and E (soft soil) (Cheng, 2002).

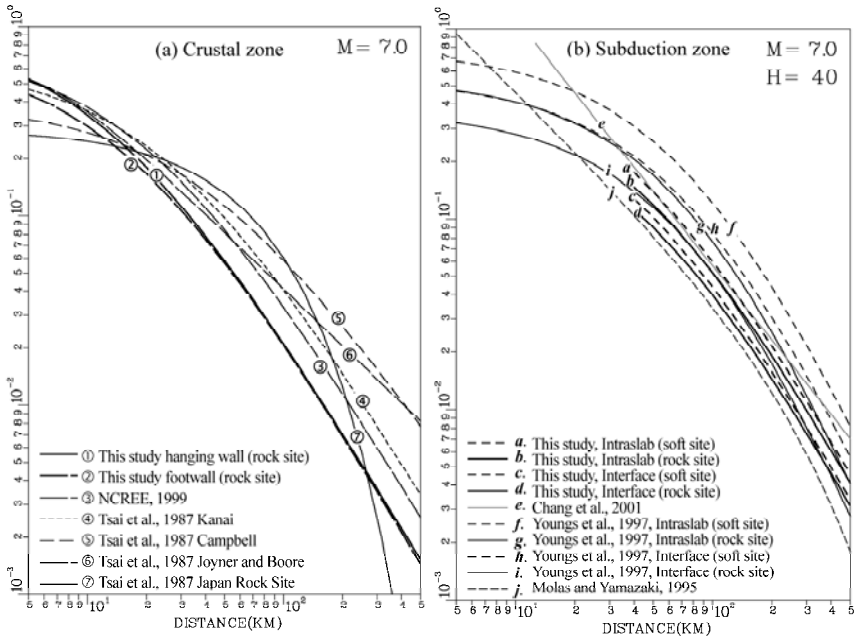

Fig. 8 The comparison of different PGA attenuation relationships for crustal and subduction zones

tionships developed by Cheng (2002) and Lin (2002) were selected magnitude in M_W, which are proper for PSHA in Taiwan region. As shown in Fig. 8, the PGA predicted by Lin (2002) is lower than that of Youngs, *et al.* (1997). It reveals that ground motion from Taiwan subduction zone source is always lower than the global data set. Also shown in Fig. 8, the HW predicts higher PGA than FW within distance less than 30 km (Cheng, 2002).

6. PSHA RESULT

The model alternatives and uncertainties were considered in the analysis to provide a computed distribution for the frequency of exceedance. The resulting distribution provides a quantitative assessment of the uncertainty in seismic hazard. The logic-tree approach has been widely used to incorporate scientific uncertainty in the PSHA (Coppersmith and Youngs, 1986; National Research Council, 1988). The logic-tree in this study shown in Fig. 9 was adopted to deal with the uncertainties of PSHA. The nodes of logic tree include source type, attenuation relationship, geometry, focal depth, magnitude distribution, earthquake recurrence, and maximum magnitude.

The GIS-based seismic hazard maps to display color-contoured ground motion values in terms of PGA in 10% (475-year return period) and 2% (2475-year return period) probability of exceedance in 50 years. The two areas with highest hazard levels in Taiwan are the eastern longitudinal valley and the western foothills to the coastal plain (as shown in Fig. 10). These two areas are separated by the central mountain range, which has a decidedly lower hazard level. After considering the fault activity and hanging wall effects in our revised PSHA, it was found that PGA levels of near-field in Taiwan always exceed 0.4 g in 475-year return period. However, in previous studies the hazard level could not be obtained because fault sources were not

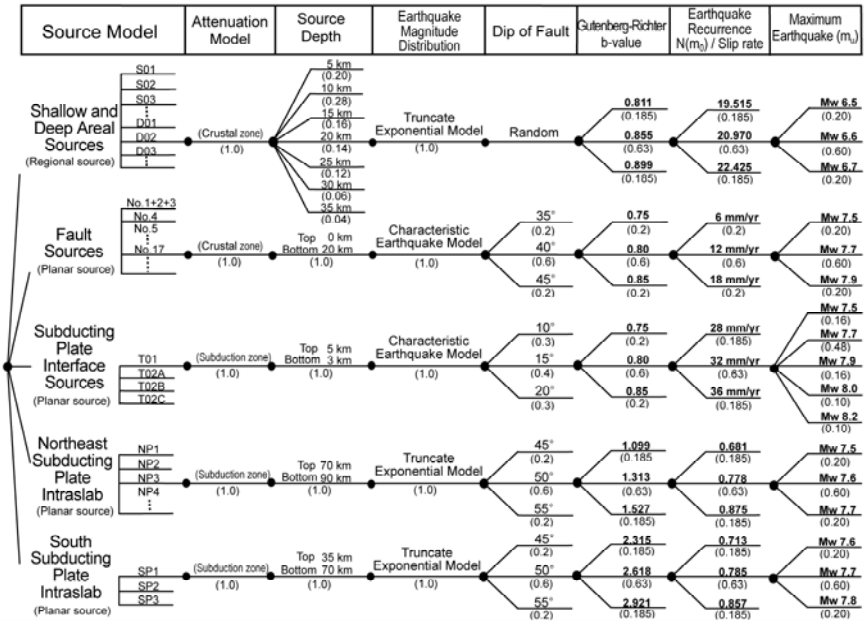

Fig. 9 Logic tree diagram for handling the uncertainty of parameters in Taiwan PSHA

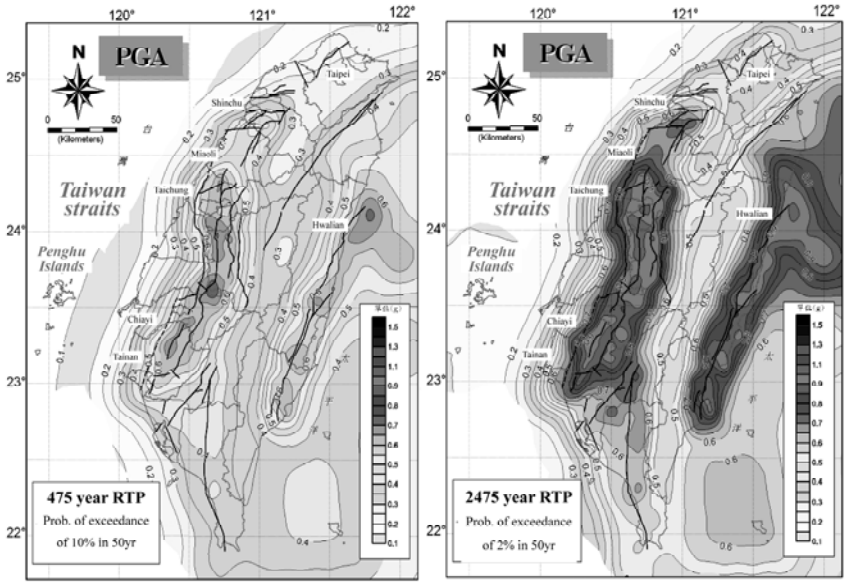

Fig. 10 Probabilistic seismic hazard maps in terms of PGA

considered, especially in long return period. This situation was very obvious in central Taiwan and the Hsinchu-Miaoli region. It has now been realized that northern Taiwan also has a much higher hazard level than previously estimated. This is due to the recognition of active faults in the vicinity and realization that subduction plate sources induce higher ground-motion levels than crustal sources.

7. DISCUSSION

In comparison with previous PSHA, the most important progresses are the consideration of active fault and new concepts of attenuation relationships after Chi-Chi earthquake. Therefore, the new attenuation relationships of ground motion need to include (1) the difference between hanging wall and footwall; (2) the difference between crust and subduction zones; and (3) site classification (Cheng, 2000). Additionally, the influence of 3-D plate fault geometry and logic-tree method for handling the uncertainties of input parameters in PSHA were also considered.

Most active faults in Taiwan are low angle thrust mechanism and their structures are very complex, epically in west coastal plain. Therefore, it is very difficult to correlate earthquakes with some specific fault system. In order to confirm the reliability of slip-rate of fault, when active faults are inside a shallow regional source, the recurrence rate of small and medium magnitude earthquake (the background seismicity, $M_W < 6.5$) in Characteristic-Earthquake model of faults must less than that in Truncated-Exponential model of shallow regional source. Further, a proper way to avoid double counting the recurrence rate of background seismicity is to treat $M_W 6.5$ as demarcation of background seismicity and large earthquake relating to a fault in this study. The fault geometries influences the seismic hazard map pattern very much, especially the fault has potential to generate large earthquake ($M_W > 6.5$) and huge rupture area. Fault rupture area of the earthquake magnitude less than $M_W 6.5$ is smaller than 150 km^2 approximately (Wells and Coppersmith, 1994). It would not influence the seismic hazard map pattern because it seems like a point source.

In previous studies, estimating the recurrence rate from the earthquake catalogs of the past century by Truncated-Exponential model, it would be unreasonable if extrapolating the recurrence rate of large earthquake from the magnitude distribution of small to medium magnitude earthquakes. It is because the recurrence interval of large earthquake induced by specific fault always several hundred years or even thousands years. Therefore, estimating the recurrence rate of large earthquake induced by fault by using Characteristic-Earthquake is more suitable model than Truncated-Exponential model.

After considering the impacts of Chi-Chi earthquake on PSHA, revised seismic hazard maps are presented. Figure 11 shows the previous study of Taiwan PSHA. It reveals that no mater what kinds of method and assumption adopted Hwalian and Tainan-Chiayi regions were always the high hazard level area. However, Tai-chung area computed in this study are higher than previously estimated, because previous analyses did not incorporate recent data on local crustal faults and the subduction zone.

8. CONCLUSIONS

This paper summarizes the framework of PSHA methodology and revises the probabilistic seismic hazard maps of Taiwan. After considering the active fault and adopting new concept attenuation relationships, it was found that the PGA levels of near-field in Taiwan always exceed 0.4 g in 475-year return period. This situation is very obvious in central Taiwan and Hsinchu-Miaoli region. In greater Taipei region, the seismic hazard is mainly contributed by nearby shallow regional sources and the northastern subduction zone sources in a 475-year return period. Furthermore, however, in a 2475-year return period, the hazard contribution is totally come from Shanchiao fault.

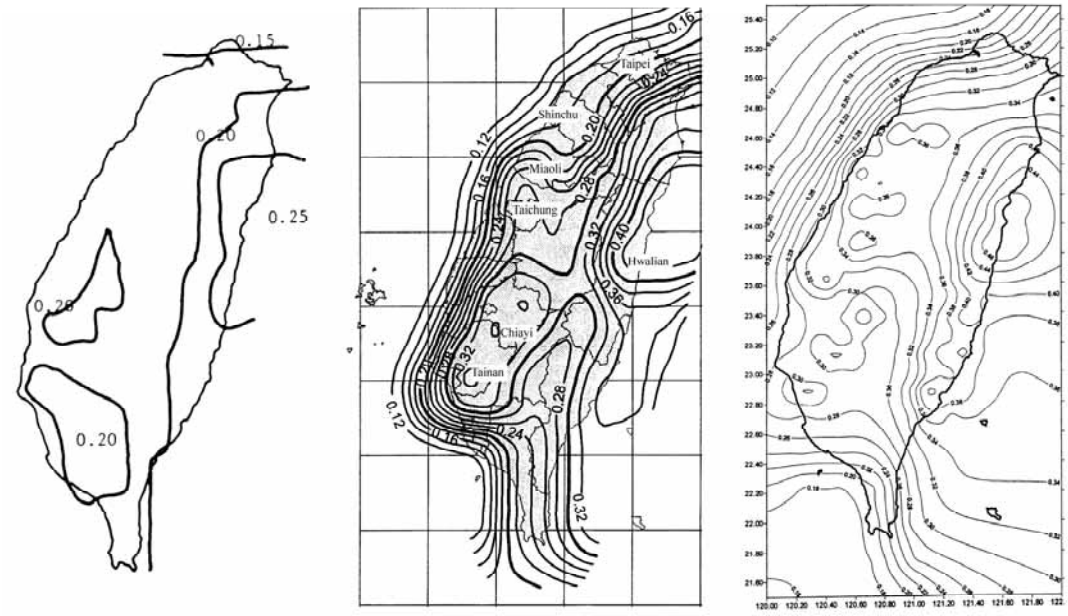

Fig. 11 Seismic hazard maps from previous studies (a) using regional sources and some fault sources; (b) use the regional sources only; (c) considering the Characteristic-Earthquake model, but not using the slip rate for estimating the seismicity rate

The eastern longitudinal valley and the western foothills to the coastal plain are the two areas with highest seismic hazard level, which may be associated with high slip-rate or high GPS horizontal velocity field of faults. Nevertheless, there are still a lot of active faults in Taiwan have no detail information for estimating more accurate slip-rate. Further studies of active faults are needed for improve seismic hazard assessment.

REFERENCES

Bollina, M. G. (1970). "Surface faulting and related effects." *Earthquake Engineering*, Wiegel, R. L., ed., Prentice-Hall, N. J., Englewood Cliffs, 47−74.

Cheng, C. T. (1997). "Seismic hazard analysis in Taiwan region based on the new seismogenic zones." M.S. Thesis, Institute of Geophysics, National Central University, Chung-Li, Taiwan (in Chinese).

Cheng, C. T. (2002). "Uncertainty analysis and de-aggregation of seismic hazard in Taiwan." Ph.D. Dissertation, Institute of Geophysics, National Central University, Chung-Li, Taiwan (in Chinese).

Cheng, S. N. and Yeh, Y. T. (1989). "Catalogue of earthquakes in Taiwan from 1604 to 1988." Institute of Earth Science, Academia Scinica (in Chinese).

Coppersmith, K. J. (1991). "Seismic source characterization for engineering seismic hazard analyses." *Proceedings, Fourth International Conference on Seismic Zonation*, Stanford University, 4, 3−60.

Coppersmith, K. J. and Youngs, R. R. (1986). "Capturing uncertainty in probabilistic seismic hazard assessments within intraplate environments." *Proceedings, Third U.S. National Conference on Earthquake Engineering*, 1, 301−312.

Cornell, C. A. (1968). "Engineering seismic risk analysis." *Bulletin of the Seismological Society of America*, 58(5), 1583−1606.

Crouse, C. (1991). "Ground-motion attenuation equations for Cascadia subduction zone earthquakes." *Earthquake Spectra*, 7, 201−236.

Earthquake Engineering Research Institute Committee on Seismic Risk (1989). "The basics of seismic risk analysis." *Earthquake Spectra*, 5, 675−702.

Fujita, L. and Kanamori, H. (1981). "Double seismic zones and stresses of intermediate depth earthquakes." *Geophysical Journal of the Royal Astronomical Society of London*, 66, 131−156.

Hetland, E. A. and Wu, F. T. (2001). "Crustal structure at the intersection of the Ryukyu Trench with the arc-continent collision in Taiwan: Results from an offshore-onshore seismic experiment." *TAO*, Supplementary Issue, 231−248.

International Conference of Building Officials (1997). *Uniform Building Code*, Whittier, California, 492.

Isacks, B. and Molnar, P. (1971). "Distribution of stresses in the descending lithosphere from a global survey of focal-mechanism solutions of mantle earthquakes." *Reviews of Geophysics and Space Physics*, 9, 103−174.

Jean, W. Y. and Loh, C. H., (1998). "A study on seismic design parameters." *Bulletin of the College of Engineering*, National Taiwan University, 73, 1−19 (in Chinese).

Jean, Z. Y. (2001). "Seismic hazard analysis and probabilistic scenario earthquakes: considering fault slip rate." M.S. Thesis, Department of Civil Engineering, National Taiwan University, Taipei, Taiwan (in Chinese).

Kao, H., Shen, S. J., and Ma, K. F. (1998). "Transition from oblique subduction to collision: earthquakes in the southernmost Ryukyu arc-Taiwan region." *Journal of Geophysical Research*, 103, 7211−7229.

Kao, H. (1998). "Can great earthquakes occur in the southernmost Ryukyu arc-Taiwan region?" *TAO*, 9, 487−508.

Kiureghian, A. D. and Ang, A. H-S. (1977). "A fault-rupture model for seismic risk analysis." *Bulletin of the Seismological Society of America*, 67(4), 1173−1194.

Lee, C. T. (1999). "Neotectonics and active faults in Taiwan." *Workshop on Disaster Prevention/Management and Green Technolgy*, Foster City, CA, U.S.A., 61−74.

Lee, C. T., Cheng, C. T., Liao, C. W., and Tsai, Y. B. (2001). "Site classification of Taiwan free-field strong-motion stations." *Bulletin of the Seismological Society of America*, 91(5), 1283−1297.

Lin, C. W., Chang, H., Lu, C. S. T., Shih, T. S., and Huang, W. J. (2000). *An Introduction to the Active Faults of Taiwan, Explanatory Text of the Active Fault Map of Taiwan*. 2nd ed., Special Pub., Central Geological Survey, MOEA, Taipei, Taiwan (in Chinese).

Lin, P. S. (2002). "Strong ground-motion attenuation relationship for subduction zone earthquakes in north-east Taiwan." M.S. Thesis, Institute of Geophysics, National Central University, Chung-Li, Taiwan (in Chinese).

Loh, C. H. and Jean, W. Y. (1993). "Uncertainty analysis in seismic hazard analysis." *Proceedings of ICOSSAR'93*, Innsbruck, Austria.

Loh, C. H., Hwang, J. Y., and Shin, T. C. (1998). "Observed variation of earthqauke motion across a basin-Taipei city." *Earthquake Spectra*, 14, 115−133.

Loh, C. H., Yeh, C. H., Chen, L. C., Hung, H. C., Jean, W. Y., and Liao, W. I. (2002). "Damage assessment system HAZ-Taiwan for seismic loss estimation in Taiwan." *Bulletin of the College of Engineering*, National Taiwan University, 85, 13−32.

Matsuda, I., Tamura, T., Mochizuki, T., and Kunii, T. (1976), "Some evidences of faulting associated with the earthquake of April 21, 1975 in the central part of Oita Prefecture." *Journal of Geography*, 85(2), 45−50 (in Japanese).

Molas, G. and Yamazaki, F. (1995). "Attenuation of earthquake ground motions in Japan including deep focus events." *Bulletin of the Seismological Society of America*, 85(5), 1343−1358.

National Research Council (1988). *Probabilistic Seismic Hazard Analysis*, National Academic Press, Washington, D.C.

National Center for Research in Earthquake Engineering (NCREE) (1999). "Damage report on 921 Chi-Chi earthquake." Report No. NCREE-99-033, Taipei, Taiwan (in Chinese).

Schwartz, D. P. and Coppersmith, K. J. (1984). "Fault behavior and characteristic earthquakes: example from the Wasatch and San Andreas fault zones." *Journal of Geophysical Research*, 89, 5681−5698.

Shyu, B., Sieh, K., Chen, Y.-G., and Liu, C.-S. (2005). "Neotectonic architecture of Taiwan and its implications for future large earthquakes." *Journal of Geophysical Research*, 110, B08402.

Tsai, Y. B. (1986). "Seismotectonics of Taiwan." *Tectonophysics*, 125, 17−37.

Tsai, C. C., Loh, C. H., and Yeh, Y. T. (1987). "Analysis of earthquake risk in Taiwan based on seismotectonic zones." *Memoir of the Geological Society of China*, 9, 413−446.

Wells, D. L. and Coppersmith, K. J. (1994). "New empirical rela-

tionships among magnitude, rupture length, rupture width, rupture area, and surface displacement." *Bulletin of the Seismological Society of America*, 84(4), 974–1002.

Youngs, R. R. and Coppersmith, K. J. (1985). "Implications of fault slip rates and earthquake recurrence models to probabilistic seismic hazard estimates." *Bulletin of the Seismological Society of America*, 75(4), 939–964.

Youngs, R. R., Chiou, S. J., Silva, W. J., and Humphrey, J. R. (1997). "Strong ground motion attenuation relationships for subduction zone earthquakes." *Seism. Res. Letters*, 68(1), 58–73.

Yeh, Y. H. and Tsai, Y. B. (1981). "Crustal structure of central Taiwan from inversion of Pwave arrival time." *Bulletin of the Institute of Earth Sciences,* Academia Sinica, 1, 83–102.

Yu, S. B., Chen, H. Y., and Kuo, L. C. (1997). "Velocity field of GPS stations in the Taiwan area." *Tectonophysics*, 274, 41–59.